N86-33005

VIRTUAL SPACE AND TWO-DIMENSIONAL EFFECTS IN PERSPECTIVE DISPLAYS

Michael Wallace McGreevy [1]
Cordell R. Ratzlaff [2]
Stephen R. Ellis [3]

ABSTRACT

When interpreting three-dimensional spatial relationships presented on a two-dimensional display surface, the viewer is required to mentally reconstruct the original information. This reconstruction is influenced by both the perspective geometry of the displayed image and the viewer's eye position relative to the display. In a study which manipulated these variables, subjects judged the azimuth direction of a target object relative to a reference object fixed in the center of a perspective display. The results support a previously developed model which predicted that the azimuth judgement error would be a sinusoidal function of stimulus azimuth. The amplitude of this function was correctly predicted to be systematically modulated by both the perspective geometry of the image and the viewer's eye position relative to the screen. Interaction of the two components of our model, the virtual space effect and the 3D-to-2D projection effect, predicted the relative amplitudes of the sinusoidal azimuth error functions for the various conditions of the experiment. Mean azimuth judgements in some directions differed by as much as 25 degrees as a result of different combinations of eye position and image geometry. Our results illustrate the need to consider the effects of perspective geometry when designing spatial information instruments, and show our model to be a reliable predictor of average performance.

INTRODUCTION

An important result of the diffusion of computer technology into aerospace applications is a growing interest in new display methods (Getty, 1982; Jauer and Quinn, 1982; Roscoe, Corl and Jensen, 1981; Warner, 1979). Imaginative airbrushed artists' conceptions of proposed pictorial displays which are to replace the instument panels of futuristic aircraft and spacecraft are increasingly common in industry publications. Some researchers have even proposed that the traditional distinction between the outside scene and the panel instruments be replaced with a virtual scene that integrates information in a new, more interpretable format, one which can be spatially configured in any desired fashion.

Whether these proposals can be transformed into practical flight instruments remains to be demonstrated, of course. The task will require that the design of spatial information displays be based on human performance measures, so that the advertised improvement in interpretability is achieved.

Many information transfer questions are raised by spatial displays, and we have attempted to address a question raised in our work on airborne traffic displays. As part of a NASA/FAA study of airborne traffic display formats, McGreevy and Ellis developed a perspective format which was shown to be superior to planview formats for separation maintainence tasks (Ellis, McGreevy, and Hitchcock, 1984). What was not clear at the time, however, was whether the particular perspective parameters we had used in our research display were optimal for accurate spatial information transfer.

[1] NASA Ames Research Center, MS 239-3, Moffett Field, CA 94035.

[2] San Jose State University, San Jose, CA 95192

[3] NASA Ames Research Center, MS 239-3, Moffett Field, CA 94035.

In an exploratory study of direction judgements in similar perspective displays, we found that azimuth error is a sinusoidal function of azimuth direction, and that the amplitude of the sinusoid is modulated by the perspective of the image. From these results, we proposed a model which seemed to be able to account for the sinusoids. That model was tested in the experiment described in this paper.

In this experiment, we tested conditions that included some which are similar to those in the previous experiment, as well as some that are very different. In particular, we made predictions based on our model for conditions in which one component of our model was literally turned upside down. The results, even in these conditions, confirm the model.

Our model consists of two components, the virtual space effect and the 3D-to-2D projection effect. These are mathematical functions which represent suspected influences on direction judgements. They are derived from a combination of image geometry, viewing geometry, and some proposed interpretive behaviors. The 3D-to-2D projection effect arises from reasonable expectation that the judged magnitude of an angle depicted in a 3D scene will be influenced by the magnitude of the 2D projection of that angle in the perspective image. The virtual space effect is the result of a hypothesized interpretive behavior in which observers of perspective images assume that the geometry of the depicted space is like that seen through a window. If, however, the eye of the observer is not at the geometrically correct point, this assumption will lead to predictable errors. The two effects comprising the model are described in detail in McGreevy and Ellis (1985). Using our model, we have predicted how the visual angle subtended by a pictorial display screen and the geometric field of view of the displayed image influence direction judgements within the displayed scene.

METHOD

Subjects

Twelve male commercial pilots ranging in age from 29 to 62 served as subjects. Their flight experience varied from 8 to 45 years. Subjects were obtained through the NASA Ames Research Center subject pool and were paid for their participation.

Apparatus and Stimuli

The stimulus images were slides of computer generated perspective scenes which were rear-projected onto a large screen (104 cm square). These images were abstracted from a spatial display format (Figure 1) that has been developed and used in air traffic display research studies at NASA Ames (McGreevy, 1982; McGreevy, 1983; Ellis, et al., 1984; McGreevy and Ellis, 1985). Stimulus scenes consisted of a grid plane and two cubes. The "reference cube" always appeared in the center of the display while the "target cube" was displayed at various positions around the reference cube. The target cube was always at the same altitude as the reference cube, and lines connected each cube to the grid, as shown in Figure 2. Ninety-six different perspective images were used in the experiment: for each of four image geometries, the target cube was depicted in twenty-four different azimuth directions.

The perspective scenes were photographed directly from an Evans & Sutherland Picture System monitor. A Kodak carousel slide projector was used to project the images onto the screen which was positioned at various distances directly in front of the subject. An adjustable chair and chinrest kept the subject's central line of sight fixed at the center of the screen while allowing the subject to sit in a comfortable position. Subjects responded by using a stylus and digitizer pad to manipulate an angle indicator dial which appeared on a computer graphics display next to the projection screen. Programs to generate the dial image and record subjects' judgements ran on a PDP-11/40 computer under the RSX-11M operating system.

Design

The experiment utilized a fully crossed, within subjects design. Each subject was presented with a total of 384 stimulus images, viewing 96 images from each of four different distances (194, 90, 52, and 30 cm). The 96 images consisted of 24 scenes, each of which was calculated with four different geometric fields of view (30°, 60°, 90°, and 120°). Each of the 24 images depicted the target cube in one of 24 azimuth directions. This design allowed each subject to view depictions of 24 different directional stimuli under 16 combinations of image geometry and viewing distance, so that the viewer made direction judgements while his

eyepoint was at four different positions relative to four different geometric station points.

Figure 3 shows all sixteen eye point/geometric station point relationships. The station point is at the apex of each of the four triangles whose base is the screen, and is defined as the point through which all projectors pass. It is the mathematical analog of a pinhole lens, through which all imaged light rays pass. The angle at the apex is the geometric field of view, which we also refer to as the geometric FOV, and is encoded in the figures as g30, for example, to label the case of a geometric field of view of 30°. The visual subtense of the screen as seen from the eye position is the eye field of view, or eye FOV, and is labelled in the diagrams as e30, etc.

Figure 4 is a three-dimensional figure which shows the geometry of a 3D scene and corresponding 2D stimulus image, which is similar to the geometries used in this experiment. Each triangle of Figure 3 represents a top-view of the tip of a frustrum like that in Figure 4, which is a geometric analog of the cone of vision.

Target cube direction was reported in terms of the azimuth angle between the zero azimuth axis and the bearing of the target cube (see Figure 2). Judgement error was defined as the difference between the actual 3D angle depicted in the display and the judged angle. A positive azimuth error represents a clockwise (CW) error, where the response is clockwise in azimuth relative to the stimulus. For example, a positive error of 10° would result if a stimulus at 60° resulted in a response of 70°. A negative azimuth error represents a counterclockwise error.

Procedure

Each subject received instructions and was shown how to operate the equipment for recording judgements. Several practice trials were administered to ensure that the subject understood the task completely. The subject wore an eye patch over his non-dominant eye and made judgements while his chin was positioned in the chinrest, allowing control over the position of the subject's eye. To reduce extreme angles of eye movement and possible strain, the subject was allowed to swivel his head in the chinrest when looking from the screen to the angle indicator dial.

The task consisted of viewing a stimulus scene, manipulating the angle in the angle indicator dial until the subject felt it best represented the angle between the two cubes in the stimulus scene, and then activating a switch to record the judgement. Immediately after the judgement was recorded, the subject was presented with the next trial. The subject received no feedback concerning the accuracy of his judgements.

The experiment was comprised of 16 blocks of 24 trials. Stimulus scenes were randomly assigned to blocks and the order in which the blocks were viewed was randomized and counterbalanced for each subject. After a subject completed a block of trials, the screen was moved to a different distance. This allowed the subject a short rest period and helped prevent eye fatigue at the closer screen distances. At the halfway point of the experiment a longer rest break was provided. Total time for the experiment was approximately three and one-half hours.

RESULTS

The ANOVA results indicate that the three-way interaction of stimulus azimuth, geometric field of view, and eye field of view is statistically significant ($F=2.051$; $df=207,2277$; $p<0.0005$). Thus, the sixteen plots of the means which correspond to the sixteen field of view conditions of the experiment (Figure 5a) are significantly dissimilar. Based on results of a previous experiment (McGreevy and Ellis, 1984; McGreevy and Ellis, 1985), we had applied the 2D effect and virtual space effect to predict the nature of the individual plots of the azimuth error means which comprise the three-way interaction. The discussion section contains a detailed comparison of the predictions and results.

The two-way interactions, which are averages across either eye FOV or geometric FOV, are less useful for validating the model, but give insight into performance which is common to a particular class of conditions. The two-way interaction of geometric FOV and stimulus azimuth (Figure 5b) is significant ($F=18.257$; $df=69,759$; $p<0.0005$). The two-way interaction of eye FOV and stimulus azimuth (Figure 5c) is also significant ($F=6.790$; $df=69,759$; $p<0.0005$).

The so-called main effect of azimuth, which is an average across both eye FOV and geometric FOV, is even less useful in terms of the model,

and is included only for completeness. The main effect of azimuth (Figure 5d) is significant ($F=2.847$; $df=23,253$; $p=0.0005$).

DISCUSSION

Error Function Equations

The plots of the three-way interaction of stimulus azimuth, geometric field of view, and eye field of view are distinctly sinusoidal. It is useful to fit analytic functions to the raw data so that the trends among the conditions of the experiment, as seen in the three-way interaction, may be described quantitatively.

In order to obtain an estimate of the shapes of the analytic functions, we fit polynomials of various degrees to the raw error data for each of the sixteen conditions of the experiment. The squared error of fit was reduced significantly for polynomials of degree greater than five, and polynomials of degree six to nine produced nearly identical plots. We used the shape of each sixth order polynomial to obtain estimates of the coefficients of a function consisting of a sine curve plus a line. These coefficients include the amplitude, frequency, and phase shift of the sine curve and the slope and intercept of the line. The estimated equations were input to a BMDPAR program (derivative-free non-linear regression) which adjusted the coefficients to obtain the "sine plus line" function for each condition which minimized the sum of the squared error of fit to the raw data.

The coefficients are shown in Tables 1-5 and are plotted next to each table, and the equations are shown in Table 6. Figure 6a shows the plots of the fitted analytic functions compared with the plots of the three-way interaction.

The **amplitudes** of the fitted sinusoidal azimuth error functions vary systematically among the conditions of the experiment (Table 1). For example, the average amplitude of the sinusoidal error is 12.34 ° when the image has a narrow geometric FOV of 30 ° (g30) and it is viewed such that it subtends a very wide visual angle of 120 ° (e120). At the other extreme, the average amplitude of the sinusoidal error is -6.72 ° when the image has a very wide geometric FOV of 120 ° (g120) and it is viewed such that it subtends a narrow visual angle of 30 ° (e30).

Notice that the minimum amplitudes of error are not obtained in those cases where the eye is at the station point (ie. when the eye FOV equals the geometric FOV). For example, when the eye FOV is 30 ° (e30), the minimum amplitude among conditions tested is obtained with a geometric FOV of 60 ° (g60). This agrees with results of our previous experiment (McGreevy and Ellis, 1984; McGreevy and Ellis, 1985).

The **angular freqency** and **phase shift** of the sinusoidal azimuth error functions determine the azimuth directions which will be the peaks and valleys of the error functions. The frequency coefficients, Table 2, seem to be randomly scattered close to a value of 2.00 cycles of error function per 360 ° of target azimuth direction, for most conditions of the experiment.

In order to compare the phase shifts of functions with negative amplitudes with those whose functions have positive amplitudes, a -90 ° shift is added to the those phase shifts whose functions have negative amplitudes. This adjustment assumes a frequency of 2.00 cycles per 360 ° of target azimuth direction. Both the adjusted and unadjusted values are shown in Table 3. Phase shift shows a distinct pattern among the conditions of the experiment. In general, the error functions are shifted in the positive azimuth direction (clockwise) for the 30 ° geometric FOV (g30), and increasingly counterclockwise for the wider geometric fields of view. The effect is most pronounced for the eye FOV of 30 ° (e30). The effect decreases and shifts to the positive direction as eye FOV increases.

The **slope** of the linear component of the sinusoidal azimuth error function is near zero for all but the case of a geometric FOV of 30 ° (g30). In this case, the slope becomes more negative as the eye FOV increases. This can also be seen in the four curves of the g30 case in Figure 6a. The **intercept** is greatest, for all geometric fields of view, when the eye FOV is 30 ° (e30) and least for the eye FOV of 120 ° (e120). Note that in cases where the slope is zero, which is approximately true for all but the g30 case, the intercept is just a 'vertical' offset of the sinusoidal azimuth error function away from the zero error line.

3D-to-2D Projection Effect

The 3D-to-2D effect, or 2D effect for short, is a geometrical relationship which, we believe, influences viewers of 2D perspective images when they make angular judgements concerning the displayed 3D space. The magnitude of the effect,

for a given angle, is equal to the difference between the 2D angle on the image plane, and the 3D angle it represents. The effect is a function of image geometry, and when the plane of the angle is constant relative to the image plane, it varies in magnitude as a function of the size of the angle and the geometric field of view. These functions are shown in Figure 6b, for the conditions and image geometry of this experiment, as dashed lines. Note that the magnitude of the effect, for a given geometric FOV, is the same for all eye fields of view, and that the effect is strongest where the geometric FOV is smallest.

Virtual Space Effect

The virtual space effect is a geometrical relationship which is based on a suspected interpretive behavior. We have proposed (McGreevy and Ellis, 1984; McGreevy and Ellis, 1985) that viewers of perspective images make what we call the "window assumption," assuming that they are at the station point, and that they then distort the 3D space, creating a virtual 3D space, to conform to that assumption. The magnitude of the effect, for a given angle, is equal to the difference between the virtual 3D angle and the actual 3D angle. It is a function of the same image parameters as the 2D effect, and is also a function of the angular difference between the eye FOV and the geometric FOV of the image. Thus, there is no virtual space effect when the eye is at the station point, and the effect increases in magnitude as the distance between the eye and station point increases. The virtual space effect functions for the conditions and image geometry of this experiment are shown as solid lines in Figure 6b.

Combined Influence of the Two Effects

When the eye is closer to the screen than the station point, as when the eye FOV is greater than the geometric FOV, the virtual space effect and the 2D effect exert influences in the same direction. In this case, we say that the two effects are **in conjunction,** and that the virtual space effect is conjunctive with the 2D effect.

When the eye is farther from the screen than the station point, as when the eye FOV is less than the geometric FOV, the virtual space effect and 2D effect exert influences in opposite directions. In this case, we say that the two effects are **in opposition,** and that the virtual space effect is opposing the 2D effect.

Since there is no virtual space effect when the eye is at the station point, only the 2D effect is influential in these cases (according to our current model).

Predictions Confirmed

We predicted that the azimuth error functions would be sinusoidal, since the 2D effect and virtual space effect are sinusoidal, and this was borne out by the results of this experiment. The angular frequency of the error function was expected to be about 2 cycles of error per 360° of stimulus azimuth, since this is the frequency of the modelled effects, and this, too, was supported by the results. The amplitudes of the sinusoidal azimuth error functions were found to agree in great detail with those predicted by the expected interplay of the 2D effect and virtual space effect.

The following discussion relates information in three figures, Figure 3, in which the eye positions and geometric station points are graphically depicted and the predicted influences are explicitly noted; Figure 6a, which has the plots of the mean errors comprising the three-way interaction of stimulus azimuth, geometric field of view, and eye field of view, as well as the fitted sinusoidal error functions; and Figure 6b, with the virtual space effect and 2D effect functions which predict the azimuth error. Note that all three of these figures are in the same spatial format so that, for example, the upper right element in each of the figures represents the condition where the geometric field of view is 30° and the eye field of view is 120°.

Eye FOV = 30°

The four conditions in which the eye FOV was 30° (e30) involved geometric fields of view of 30° (g30), 60° (g60), 90° (g90), and 120° (g120). This set of conditions is quite similar to that used in our previous experiment, where the geometric fields of view were the same and the eye field of view was 18°; the results confirm those of the previous study. The amplitude of the error function is large and positive (6.82° error) when both the eye FOV and the geometric FOV are 30° (e30,g30), since the 2D effect is strong and the virtual space effect is zero. As the geometric FOV increases, the amplitude decreases, then reverses in sign, and then increases in the negative direction since the 2D effect becomes weaker and is gradually overcome by the increasing strength of the opposing virtual

space effect. Finally, when the geometric FOV reaches 120° (g120), with the eye FOV still 30° (e30), the amplitude of the error function reaches its largest negative value (-6.72° error), since the 2D effect is weakest and the opposing virtual space effect is strongest in this condition.

Eye FOV = 120°

The largest positive amplitude (12.34° error) of the sinusoidal error function occurs, as predicted, when the geometric FOV is 30° (g30) and the eye FOV is 120° (e120), since both the the 2D effect and the conjunctive virtual space effect are at their strongest. As the geometric FOV increases, with the eye FOV still 120°, the amplitude of the error function decreases since both the 2D effect and the conjunctive virtual space effect become weaker. Finally, when the geometric FOV reaches 120° (g120), with the eye FOV still 120° (e120), the amplitude is very small (1.97° error) since the virtual space effect is zero and the 2D effect is at its weakest.

Geometric FOV = 30°

In the set of conditions for which the geometric FOV is 30° (g30) and the eye FOV has values of 30° (e30), 60° (e60), 90° (e90), and 120° (e120), the 2D effect is at its strongest. Error amplitude changes from a large positive value (6.82° error) when the eye FOV is 30° (e30), to a very large positive value (12.34° error) when the eye FOV is 120°. This is as predicted, since the increasingly strong conjunctive virtual space effect adds its influence to the already strong 2D effect.

Geometric FOV = 120°

In the set of conditions for which the geometric FOV is 120° (g120) and the eye FOV has values of 30° (e30), 60° (e60), 90° (e90), and 120° (e120), the 2D effect is at its weakest. Error amplitude diminishes from a large negative value (-6.72° error) when the eye FOV is 30° (e30), to a small value (1.97° error) when the eye FOV is 120°. This is as predicted, since the gradually weakening magnitude of the opposing virtual space effect adds its influence to the weak 2D effect.

Eye FOV = Geometric FOV

In the four conditions where the eye FOV is the same as the geometric FOV the eye is positioned at the station point. For this reason, the virtual space effect is zero and only the 2D effect is influential. The largest error amplitude occurs when eye FOV and geometric FOV are both 30° since the 2D effect is strong when the geometric FOV is 30°. As both the geometric and the eye fields of view increase to 120°, the error amplitude decreases since the 2D effect becomes weaker as the geometric FOV approaches 120°.

Other Issues

In the two cases where the magnitudes of the opposing virtual space effect and the 2D effect are nearly identical, the greater strength of the 2D effect overcomes the opposition. These two conditions are those where the geometric FOV is 60° and the eye FOV is 30° (g60,e30) and where the geometric FOV is 90° and the eye FOV is 60° (g90,e60).

In our previous experiment, we found that the 2D and virtual space effect functions better matched the error data when they were both shifted counter-clockwise 22°. We suspected that this was caused by the fact that our zero azimuth axis, from which 3D azimuth judgements were measured, was rotated 22° counter-clockwise from straight ahead into the depicted scene. For that reason, we tried the opposite rotation in this experiment, and correctly predicted that the 2D and virtual space effect functions would best represent expected errors if they were correspondingly shifted 22° clockwise. This is how the two effects are plotted in Figure 6a.

Exceptions

While all of the predictions above apply to variations in the amplitude of the error function, no prediction was made regarding the optimum combination of the 2D effect and the virtual space effect. We have assumed, based on previous experimental results, that the two effects have positive weights, and that they are additive in some sense. It would appear that the relative weights of the two effects vary with stimulus azimuth. For example, in the condition where the geometric FOV is 30° and the eye FOV is 120° (see Figure 6), we correctly predicted that the two effects would combine to produce a sinusoidal error function with a large amplitude, but it is clear that the *varying* amplitude of the virtual space effect is not reflected in the data.

SUMMARY

Pictorial spatial instruments will continue to emerge in aerospace applications. Advanced computational and display technology will provide a *tabula rasa* for display designers with great potential for improvement in human-machine interaction. This great freedom, however, creates new and more difficult questions about information transfer. As more onboard systems are automated, mission operators will require a different class of instruments than those traditionally† used, in order to maintain overall situational awareness in complex and dynamic operational environments.

Our work in airborne traffic display research led us to study spatial information transfer issues related to the use of perspective display formats. In particular, we have studied how within-display-space direction judgements are affected by perspective geometry. We discovered that azimuth error is a sinusoidal function of stimulus azimuth and that the amplitude of the error function is modulated by the perspective of the image and the viewer's eye position relative to the display. To explain this result, we have developed a model which combines virtual space and 3D-to-2D projection effects. In this experiment, the model has been shown to be a reliable predictor of the amplitude of the error function under a wide variety of image geometries and viewing conditions.

ACKNOWLEDGEMENTS

The authors wish to thank Amy Wu of Informatics General Corporation for her very helpful systems and programming support. She continues to be a valued and appreciated member of our research team.

REFERENCES

Ellis, S. R., McGreevy, M. W., and Hitchcock, Robert J. (1984, April). Influence of a perspective cockpit traffic display format on pilot avoidance maneuvers. In *Proceedings of the AGARD Aerospace Medical Panel Symposium on Human Factors Considerations in High Performance Aircraft.* Williamsburg, Virginia.

Getty, D.J. (Ed.). (1982, January). *3-D Displays: Perceptual research and applications to military systems.* Washington, D.C.: National Academy of Sciences.

Jauer, R.A., and Quinn, T.J. (1982, February). *Pictorial formats, vol 1: Format development* (Tech. Report AFWAL-TR-81-3156). Wright-Patterson AFB, OH: Flight Dynamics Laboratory.

Jones, L.F., Schrader, H.J., and Marshall, J.N. (1950, April). Pictorial display in aircraft navigation and landing. *Proceedings of the I.R.E.,* 391-400.

McGreevy, M.W. (1982, June). A perspective display of air traffic for the cockpit. In *Proceedings of the 18th Annual Conference on Manual Control* (pp. 514-521). (Tech. Report AFWAL-TR-83-3021), Wright-Patterson AFB, OH: Flight Dynamics Laboratory.

McGreevy, M.W. (1983). *A perspective display of air traffic for the cockpit.* Unpublished M.S. Report, University of California, Berkeley.

McGreevy, M.W., and Ellis, S.R. (1984, June). Direction judgement errors in perspective displays. In *Proceedings of the 20th Annual Conference on Manual Control* (pp. 531-549). NASA Conference Publication 2341.

McGreevy, M.W., and Ellis, S.R., (1985). *Format and basic geometry of a perspective display of air traffic for the cockpit.* (Tech. Memorandum 86680). Moffett Field, CA: NASA Ames Research Center, Aerospace Human Factors Research Division.

McGreevy, M.W., and Ellis, S.R., (1985). *The effect of perspective geometry on judged direction in spatial information instruments.* Submitted for publication.

Roscoe, S.N., Corl, L., and Jensen, R.S. (1981, June). Flight display dynamics revisited. *Human Factors, 23,* 341-353.

Warner, D.A. (1979, June). *Flight path displays* (Tech. Report AFFDL-TR-79-3075), Wright-Patterson Air Force Base, OH: Flight Dynamics Laboratory.

† For an early pictorial instrument idea which was ahead of the technology, see Jones, Schrader, and Marshall, 1950.

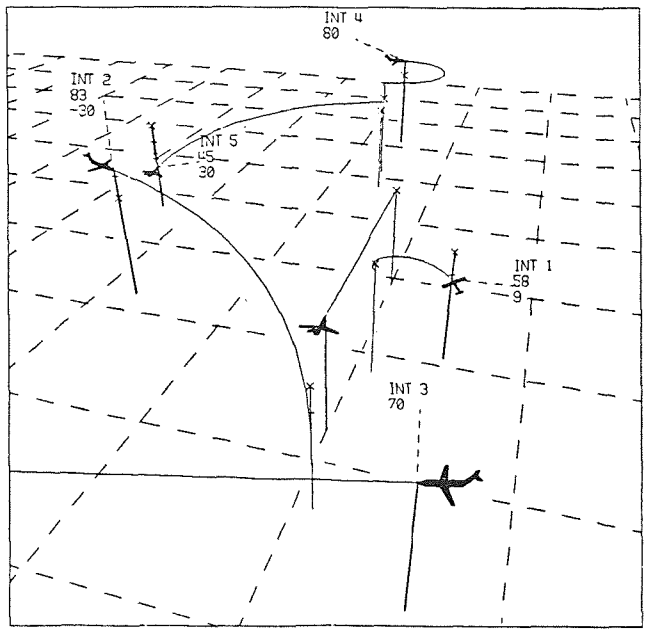

Figure 1. A perspective display of air traffic for the cockpit with ownship shown at the center of the image.

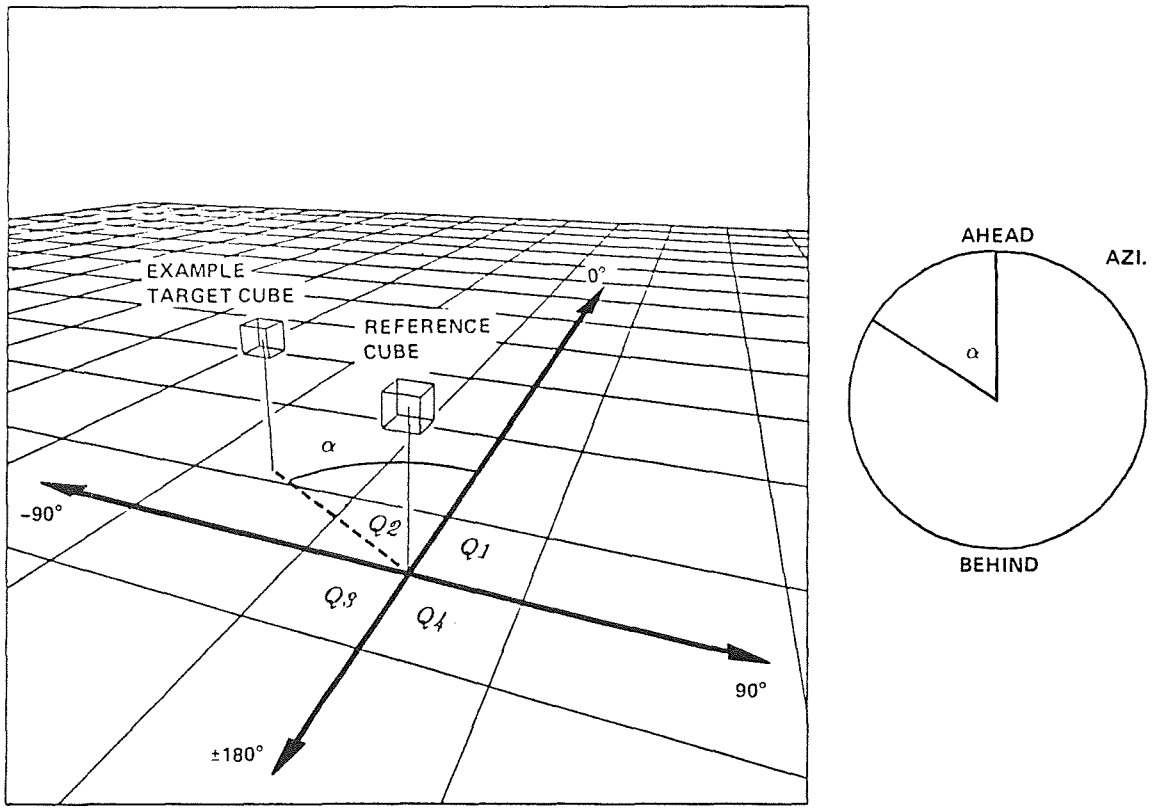

Figure 2. Diagram of a typical stimulus image. Bold axis lines, dashed line, angle arc, and text were not included in actual stimulus images. Response dial appeared on a separate screen.

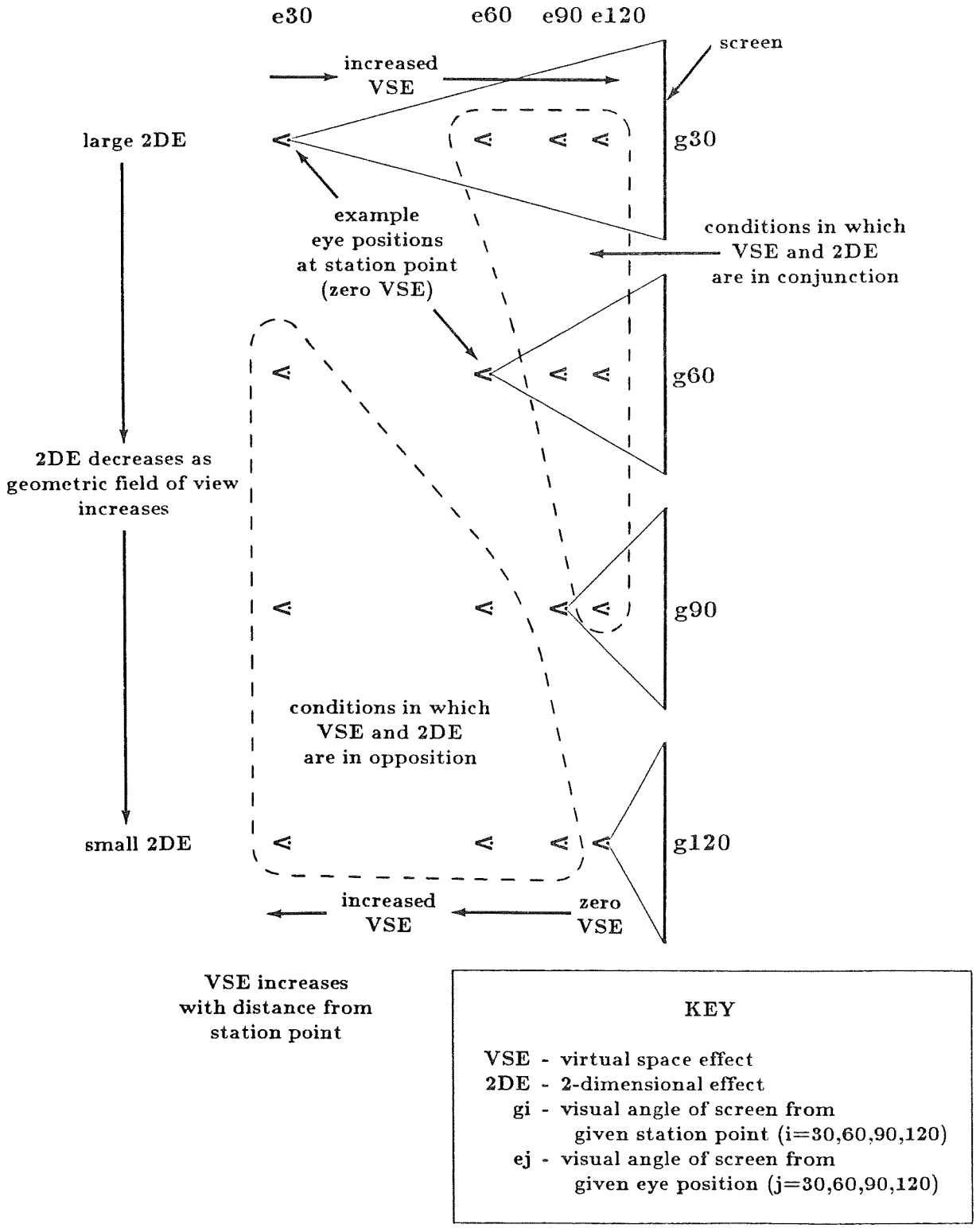

Figure 3. Conditions of the experiment: eye positions are crossed with geometric fields of view and shown relative to the screen (drawn to scale).

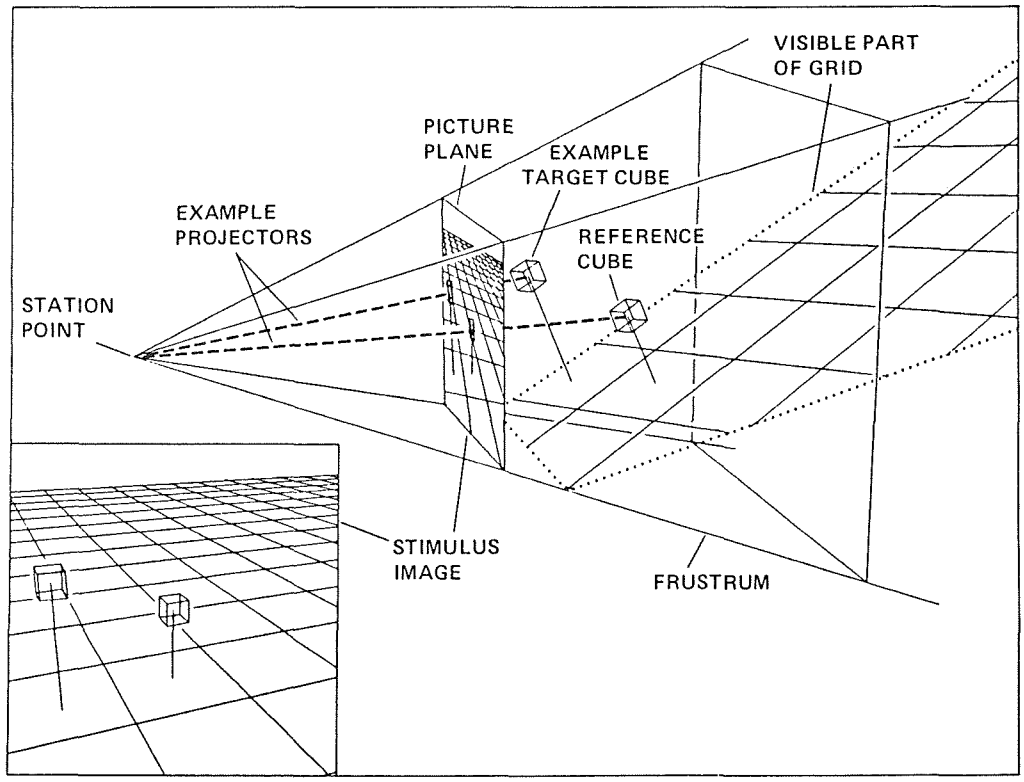

Figure 4. Example stimulus geometry showing relationship between 3D information and 2D projection.

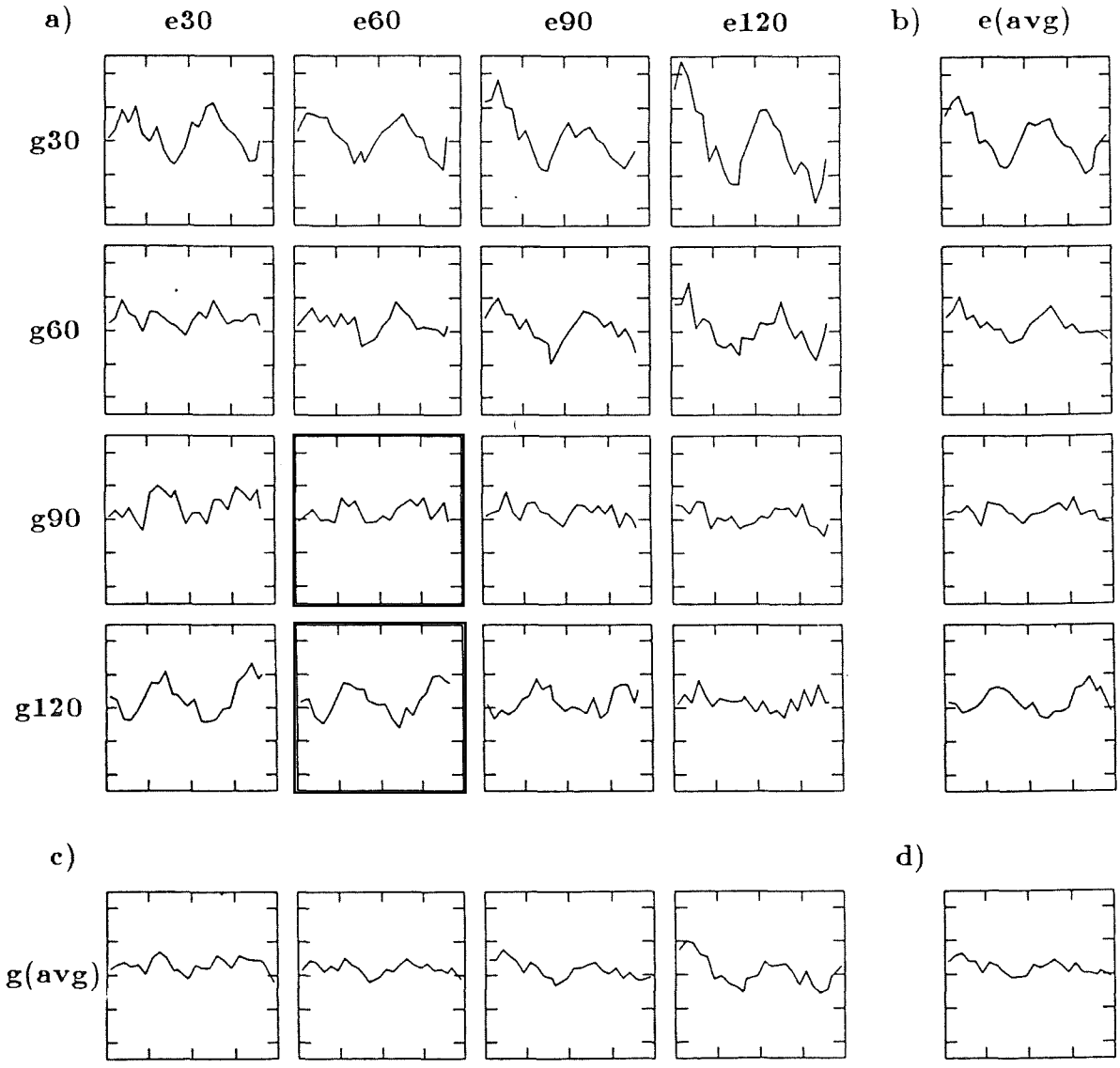

KEY

a) Three-way interaction of eye field of view, geometric field of view, and stimulus azimuth

b) Two-way interaction of geometric field of view and stimulus azimuth

c) Two-way interaction of eye field of view and stimulus azimuth

d) Main effect of stimulus azimuth

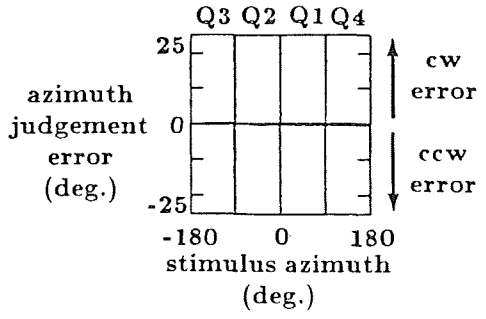

Figure 5. Average azimuth judgement error as a function of stimulus azimuth for the various perspective and viewing conditions of the experiment. Quadrants labelled in key correspond to those in Figure 2.

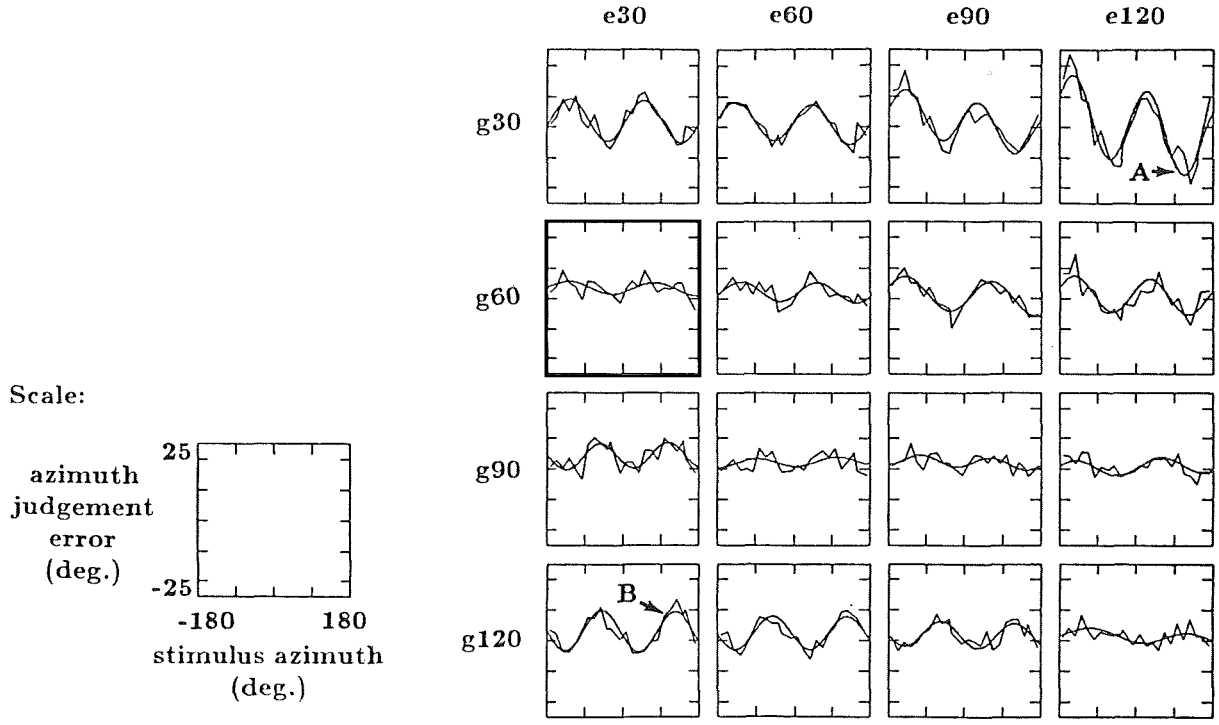

Figure 6a. Mean azimuth error and fitted functions. Note that errors at A and B differ by about 25 degrees.

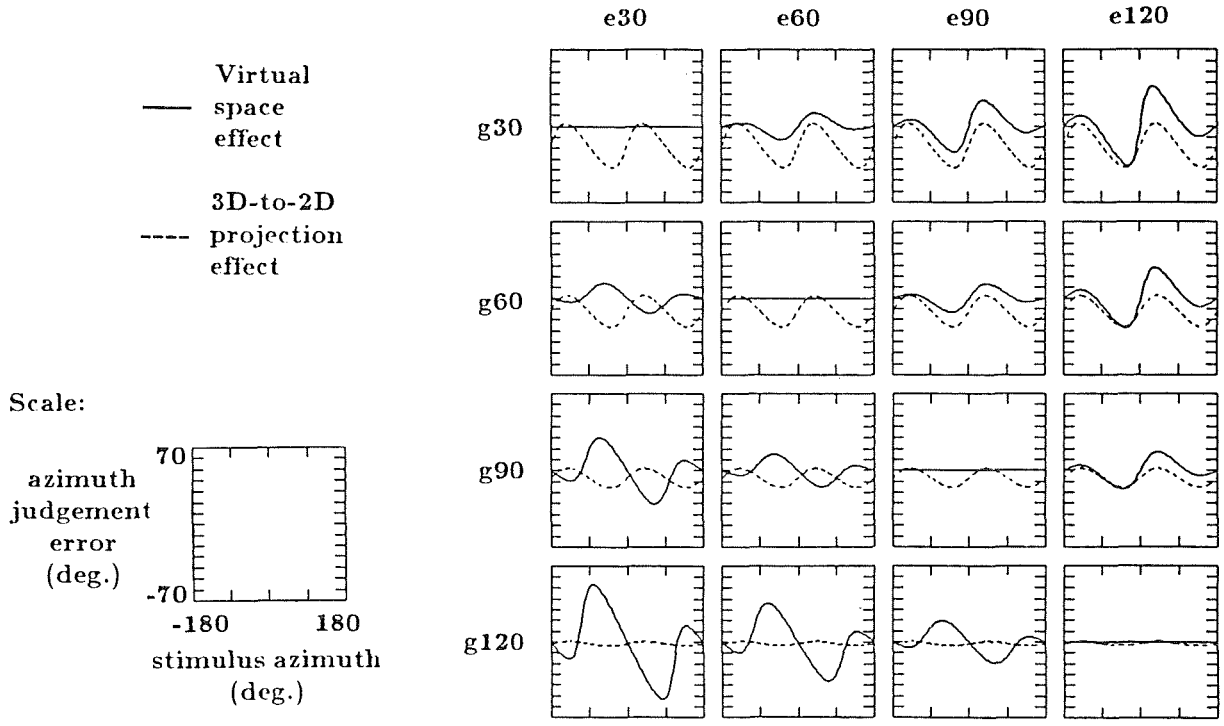

Figure 6b. Virtual space effect and 3D-to-2D projection effect difference functions for conditions of the experiment.

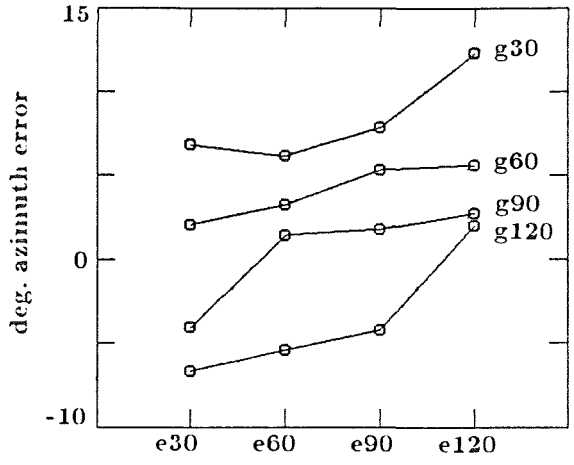

Table 1. Amplitude.

FOV	e30	e60	e90	e120
g30	6.82	6.15	7.28	12.34
g60	2.01	3.23	5.30	5.72
g90	-4.06	1.41	1.73	2.72
g120	-6.72	-5.45	-4.25	1.97

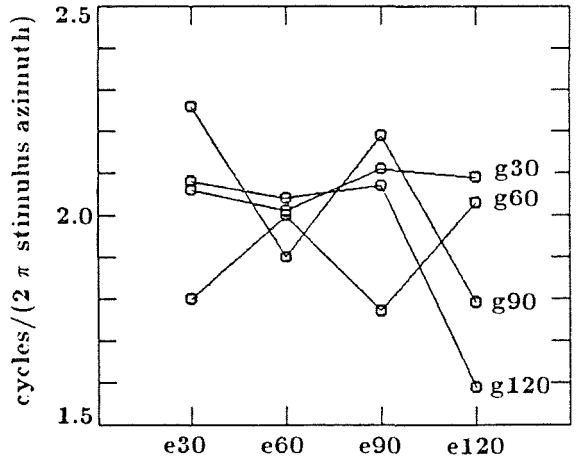

Table 2. Frequency.

FOV	e30	e60	e90	e120
g30	2.06	2.01	2.11	2.09
g60	1.80	2.00	1.77	2.03
g90	2.26	1.90	2.19	1.79
g120	2.08	2.04	2.07	1.59

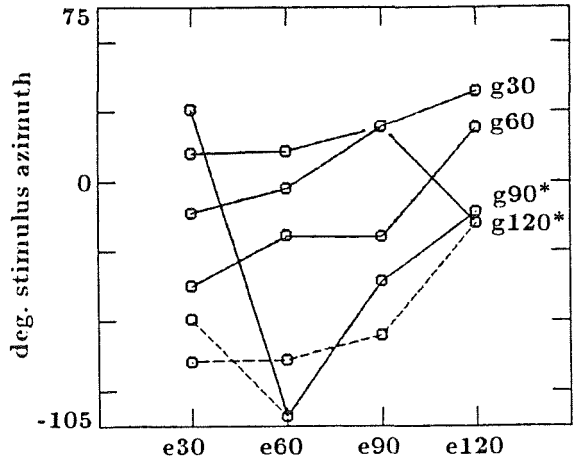

Table 3. Phase shift.

FOV	e30	e60	e90	e120
g30	-13.46	-3.04	23.61	38.85
g60	-44.92	-23.43	-24.06	23.09
g90*	30.83 (-59.17)	-101.07	-43.37	-13.06
g120*	12.38 (-77.62)	12.95 (-77.05)	23.66 (-66.34)	-17.98

* Numbers in parentheses and dashed graph lines represent alternative phase shift values for conditions in which negative amplitude values were obtained (See amplitude table). These alternative values are provided to facilitate comparison between phase shift values.

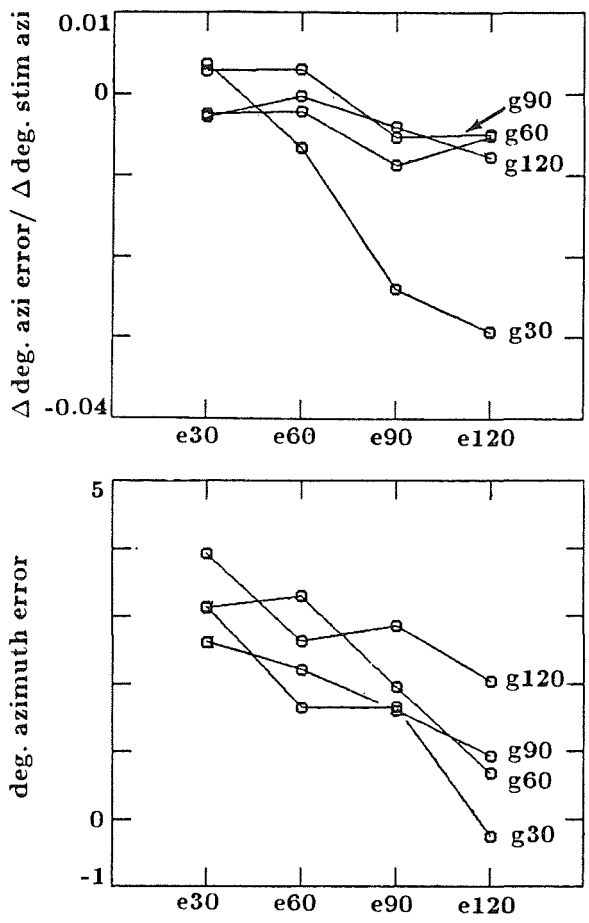

Table 4. Slope.

FOV	e30	e60	e90	e120
g30	0.0036	-0.0066	-0.0240	-0.0294
g60	-0.0025	-0.0022	-0.0087	-0.0052
g90	0.0027	0.0030	-0.0053	-0.0050
g120	-0.0028	-0.0003	-0.0041	-0.0077

Table 5. Intercept.

FOV	e30	e60	e90	e120
g30	1.95	1.14	1.37	0.08
g60	3.31	2.04	0.71	0.87
g90	4.25	2.33	2.35	0.86
g120	3.06	2.39	1.79	1.38

Table 6. Sinusoidal azimuth error functions for all eye point/geometric station point conditions. θ = stimulus azimuth.

$$
\begin{aligned}
f(g30,e30,\theta) &= 6.82\sin(2.06\theta - 13.46) + 0.0036\theta + 1.95\\
f(g30,e60,\theta) &= 6.15\sin(2.01\theta - 3.04) - 0.0066\theta + 1.14\\
f(g30,e90,\theta) &= 7.28\sin(2.11\theta + 23.61) - 0.0240\theta + 1.37\\
f(g30,e120,\theta) &= 12.24\sin(2.09\theta + 38.85) - 0.0294\theta + 0.08\\
\\
f(g60,e30,\theta) &= 2.01\sin(1.80\theta - 44.92) - 0.0025\theta + 3.31\\
f(g60,e60,\theta) &= 3.23\sin(2.00\theta - 23.43) - 0.0022\theta + 2.04\\
f(g60,e90,\theta) &= 5.30\sin(1.77\theta - 24.06) - 0.0087\theta + 0.71\\
f(g60,e120,\theta) &= 5.72\sin(2.03\theta + 23.09) - 0.0052\theta + 0.87\\
\\
f(g90,e30,\theta) &= -4.06\sin(2.26\theta + 30.83) + 0.0027\theta + 4.25\\
f(g90,e60,\theta) &= 1.41\sin(1.90\theta - 101.07) + 0.0030\theta + 2.33\\
f(g90,e90,\theta) &= 1.73\sin(2.19\theta - 43.37) - 0.0053\theta + 2.35\\
f(g90,e120,\theta) &= 2.72\sin(1.79\theta - 13.06) - 0.0050\theta + 0.86\\
\\
f(g120,e30,\theta) &= -6.72\sin(2.01\theta + 12.38) - 0.0028\theta + 3.01\\
f(g120,e60,\theta) &= -5.45\sin(2.04\theta + 12.95) - 0.0003\theta + 2.39\\
f(g120,e90,\theta) &= -4.25\sin(2.07\theta + 23.66) - 0.0041\theta + 1.79\\
f(g120,e120,\theta) &= 1.97\sin(1.59\theta - 17.98) - 0.0077\theta + 1.38
\end{aligned}
$$